Effects of Different Advanced Engineering Materials on Deformation Behaviour of Wood Structural Materials

Timucin Bardak *

Wooden composites reinforced with advanced engineering materials are promising as building materials. The use of these materials has been increasing in recent years. It is important to understand the behaviour of their deformation under load for optimum design of composite materials. There is limited information about the deformation behaviour of wooden composites under different loads. In this study, strain and displacement distributions were measured for wood structural materials made with glass fibre, carbon fibre, oak (*Quercus robur*), and polyurethane resin. The digital image correlation method (DIC) was used for this purpose. Deformation behaviours were determined from the images recorded under specific loads in the bending test. There was an increase of 17.3% in bending strength of wood composites with the addition of glass fiber. The cracking process was visualized for different advanced engineering materials. The imagery clearly showed the development of the strain and displacement field. The deformation behaviours of reinforced and unreinforced wood composites were different. The strain distribution of wood composites significantly affected the strength properties.

Keywords: Wooden composites; Digital images; Structural materials; Deformation; Strain measurement

*Contact information: Furniture and Decoration Program, Bartin Vocational School, Bartin University, 74000, Bartin, Turkey; *Corresponding author: timucinb@bartin.edu.tr*

INTRODUCTION

Wood is a strong, enduring, and renewable raw material (Hu *et al*. 2015). However, wood composites have poor load-carrying capacity compared with concrete and steel (Dunlop and Fratzl 2013; Zhou *et al*. 2015). In recent years, fibre-reinforced elements have been widely used to strengthen wood structural materials, as they present a significant strength increase with minimal encumbrance and mass increase (Ianasi 2015; Tekieli *et al*. 2017). Additionally, the costs of synthetic fibres are rapidly decreasing (Wei *et al*. 2013). Evaluation of the mechanical behaviour of wooden structures is important for both design and durability. Strain and displacement parameters should be properly addressed in construction projects.

Optical methods are frequently used to analyze engineering problems (Valle *et al*. 2018). In the field of solid mechanics, it is important to know the deformation behaviours that occur on the surface of inspected materials (Yoneyama *et al*. 2016). Digital image correlation (DIC) is a method to characterize various aspects of wood displacement, crack tips, and strain fields (Ling *et al*. 2009). Digital image correlation is based on the correlation of grey values of successive digital images of the undeformed and the deformed specimen (Sutton *et al*. 1988; Shen *et al*. 2015). It is widely used in mechanical engineering and provides advanced information (Pan *et al*. 2009; Caminero *et al*. 2014; Tekieli *et al*. 2017). This method allows measurements over the entire surface of the examined specimen, far

beyond a limited number of distinct points (Mahal *et al*. 2015). Furthermore, the cumulative crack openings of microcracks present in the material can be clearly defined (Luo *et al*. 1993; Alam *et al*. 2014). Digital image correlation has been applied to measure the mechanical features of wood (Serrano and Enquist 2005; Ljungdahl *et al*. 2006; Sjödin *et al*. 2006; Jeong and Park 2016; Bardak *et al.* 2017). However, there has been limited study to assess deformation behaviours of wood composite materials based on DIC.

This study investigated the effects of different advanced engineering materials on strain and displacement distributions of wooden composites. Moreover, cracking profiles were determined. Open source two-dimensional (2D) DIC software (Ncorr) was employed to determine the whole field displacements under specific loads in the bending tests (Blaber *et al*. 2015). The DIC method appears to be a suitable method for analyzing and describing deformations in wood composites reinforced with advanced engineering materials. The results showed that deformation behaviours of carbon- and glass-reinforced wood composites were different from those of wood composites without reinforcement. Moreover, the impact on bending strength of advanced engineering materials was determined. The highest bending strength values were found in glass fibre-reinforced composites.

EXPERIMENTAL

The research consisted of two main stages: The experimental bending test of the samples, followed by the analysis of the displacement and strain of the samples from the images obtained by the digital camera.

Material and Testing

Two different reinforced (carbon fibre, glass fibre) wooden composites and unreinforced wooden composite were tested in the bending test. We used carbon and glass fibres, having bidirectional fibres network in study. Carbon and glass fibres had a thickness of 0.25 mm. Table 1 presents the mechanical properties of the glass fibre and carbon fibre used in experiment.

Table 1. Mechanical Properties of the Glass and Carbon Fibres

Material	Tensile Strength (MPa)	Young's Modulus (GPa)	Density (g/cm^3)	Colour
Glass fibre	1200	80	2.5	white
Carbon fibre	2100	175	2.0	black

Before the test, wood (*Quercus robur*) samples were prepared in a climate-controlled room. Temperature and relative humidity were adjusted to 20 °C and 50%, respectively. The specific weight of the wood used in the study was 0.67 g/cm^3. In the bending test, modulus of rupture (MOR) and modulus of elasticity (MOE) of the wood material were 85 MPa and 11950 MPa, respectively. The composites were produced separately using polyurethane adhesive with carbon and glass fibres. A pressure of 0.8 N/mm^2 was applied to the composites for 4 h. The wooden composites were 330 mm long with rectangular cross sections of 50 mm × 40 mm. Figure 1 illustrates the wood composites used in the experiment. All the composites were used with a layer of reinforcing material. The weight ratio between adhesive and carbon fibre was 0.84. And the weight

ratio between adhesive and glass fibre was 0.60. The adhesive layer had a mean thicknesses of approximately 0.15 mm in all composites. Table 2 shows the properties of the wood composites.

Table 2. Properties of Wood Composites

Sample Code	Wooden Material	Adhesive	Reinforcement Material	Number of Samples
UC	Oak (*Quercus robur*)	Polyurethane	Unreinforced	10
CC	Oak (*Quercus robur*)	Polyurethane	Carbon fibre	10
GC	Oak (*Quercus robur*)	Polyurethane	Glass fibre	10

Bending strengths of the wooden composites were determined according to the TS 2474 standard (1976). The distance between the centers of the two supports was 300 mm free span. The wood composites were aimed to achieve failure in 300 ± 50 s. For each wooden composite, ten tests were made in the bending test. Statistical analysis of the results was made using ANOVA of SPSS software (IBM Corporation, New York, USA).

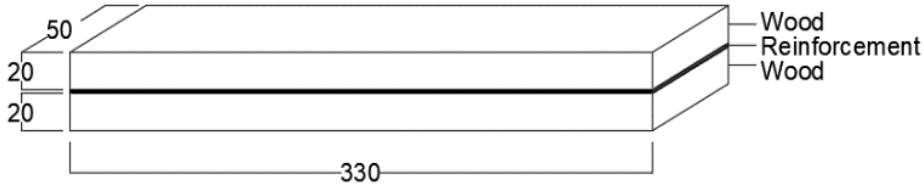

Fig. 1. The wood composite used in the experiment

Digital Image Correlation

Digital image correlation is a non-contact method popularly used for measuring deformation based on speckle patterns (Pan *et al*. 2009; Vora *et al*. 2018). It gives important information about deformations of materials. To examine displacement, strain, and fracture distribution on the reinforced (carbon fibre, glass fibre) and unreinforced wooden composites, bending tests were performed using a universal testing machine equipped with LabVIEW (National Instruments, Austin, TX, USA), Ncorr software, and a digital camera measurement system (Nguyen *et al*. 2017). Figure 2 shows the experimental setup for the 2D DIC method.

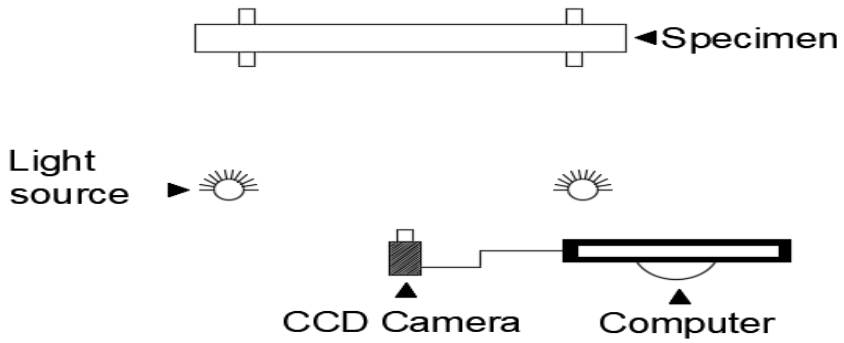

Fig. 2. The experimental setup for the 2D DIC method

LabVIEW software was used to acquire and prepare images (Hryniewicz *et al*. 2015). This software is a visual programming language. It is popular and easy to use, compared to other programming languages (Mahmoodi *et al*. 2018).

The camera (Basler ace acA1600-20gc) had a resolution equal to 1626 pixels × 1236 pixels. The camera was used to record the entire surface image of the composites in 24-bit RGB colour and 1624 pixel × 1234 pixel resolution JPEG format (.jpg). Deformation was determined using open source code and MATLAB-based Ncoor software (Harilal *et al*. 2015).

RESULTS AND DISCUSSION

Static Bending Test

The main purpose of this study was to analyze strain and displacement distributions caused by fracture in the wood composite samples with DIC. Table 3 shows measured values of force for non-reinforced wood composites (UC), the wood composites reinforced with carbon fibre (CC), and the wood composites reinforced with glass fibre (GC).

Table 3. Bending Strengths of the Composites

Code	Bending Strength (N/mm^2)	Duncan*	Standard Deviation
UC	54.60	A**	4.77
CC	52.80	A	4.44
GC	64.20	B	3.56

* Duncan's multiple range test was performed.
** Rows with the same letter do not differ statistically ($p < 0.05$).

The bending strength of the wood composites was increased with the addition of glass fibre by 17.6% compared with the unreinforced composites. The results were consistent with previous studies (Thorhallsson *et al*. 2017). However, carbon fibre did not increase the bending strength.

The lack of significant bending strength increase in carbon fibre-reinforced composites can be explained by the low strength of the interface between wood and carbon fibre (Tavakkolizadeh and Saadatmanesh 2001).

Measurement of Displacement and Strain

The DIC method is an effective means of measuring deformation behaviour (Li *et al*. 2013). The fields of displacement and strain give a general overview of the efforts that occur in the structure (Bigaud *et al*. 2018).

Bending tests were carried out on different types of unreinforced wood composites (UC), wood composites reinforced with carbon fibre (CC), and wood composites reinforced with glass fibre (GC). Their displacement/strain maps were compared. Figure 3 shows the load-displacement curves of all wood composites based on the results obtained from the experimental and DIC method.

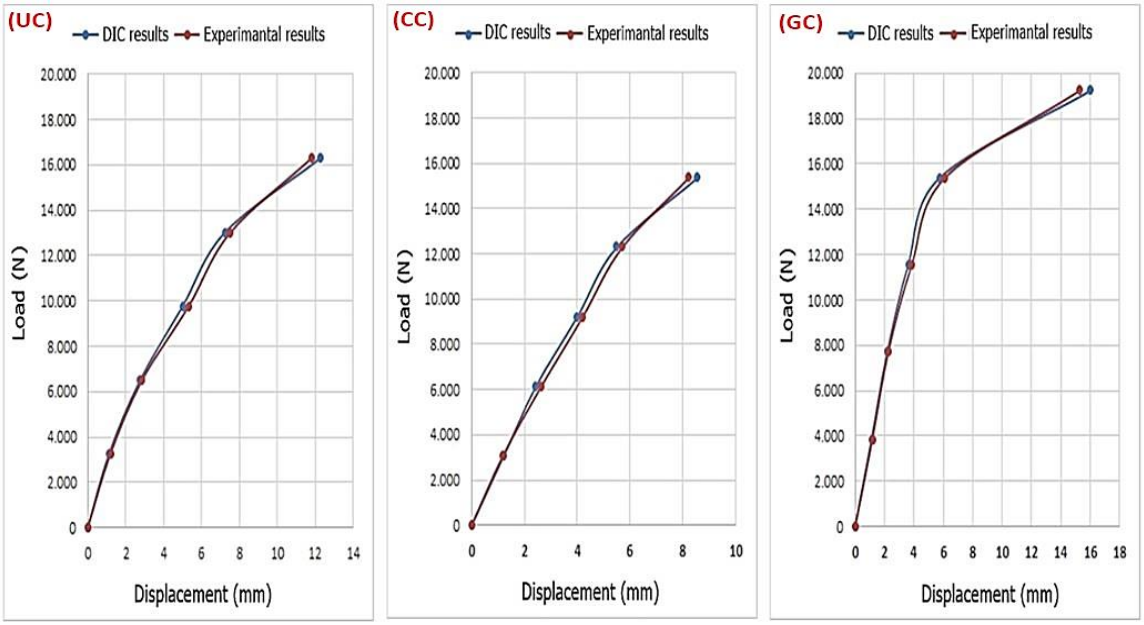

Fig. 3. The load-displacement curves of all wood composites based on the results obtained from the experimental and DIC method.

Table 4 shows deformation and strain values for the wood composites.

Table 4. Deformation and Strain Values for Wood Composites

		Maximum Applied Force (F_{MAX})									
		20% of F_{MAX}		40% of F_{MAX}		60% of F_{MAX}		80% of F_{MAX}		100% of F_{MAX}	
	Sample Code	max	min	max	min	max	min	max	min	max	min
U (mm)	UC	0.351	0.053	0.570	-0.080	0.801	-0.188	0.962	-0.369	2.284	-1.433
	CC	0.082	-0.406	0.063	-0.706	0.196	-0.884	0.390	-1.023	0.815	-1.393
	GC	0.379	0.001	0.471	-0.057	0.612	-0.125	0.818	-0.229	2.398	-2.048
V (mm)	UC	1.115	0.086	2.764	0.425	5.008	0.987	7.243	1.338	12.253	0.440
	CC	1.219	0.010	2.436	0.081	4.001	0.157	5.493	0.230	8.553	-0.066
	GC	1.112	0.215	2.185	0.421	3.619	0.724	5.703	0.987	16.037	-1.269
Ɛxx	UC	0.003	-0.002	0.005	-0.002	0.004	-0.004	0.006	-0.007	0.101	-0.017
	CC	0.002	-0.003	0.002	-0.005	0.004	-0.007	0.005	-0.009	0.005	-0.013
	GC	0.002	-0.002	0.003	-0.002	0.003	-0.002	0.004	-0.005	0.027	-0.027
Ɛxy	UC	0.003	-0.001	0.005	-0.003	0.007	-0.006	0.011	-0.009	0.018	-0.049
	CC	0.004	-0.006	0.006	-0.010	0.009	-0.015	0.011	-0.021	0.023	-0.029
	GC	0.002	-0.002	0.003	-0.004	0.005	-0.005	0.008	-0.009	0.055	-0.033
Ɛyy	UC	0.001	-0.003	0.001	-0.007	0.002	-0.016	0.003	-0.026	0.029	-0.042
	CC	0.001	-0.013	0.001	-0.019	0.001	-0.030	0.002	-0.043	0.004	-0.061
	GC	0.001	-0.005	0.000	-0.006	0.001	-0.010	0.001	-0.020	0.029	-0.637

Max = maximum, min = minimum

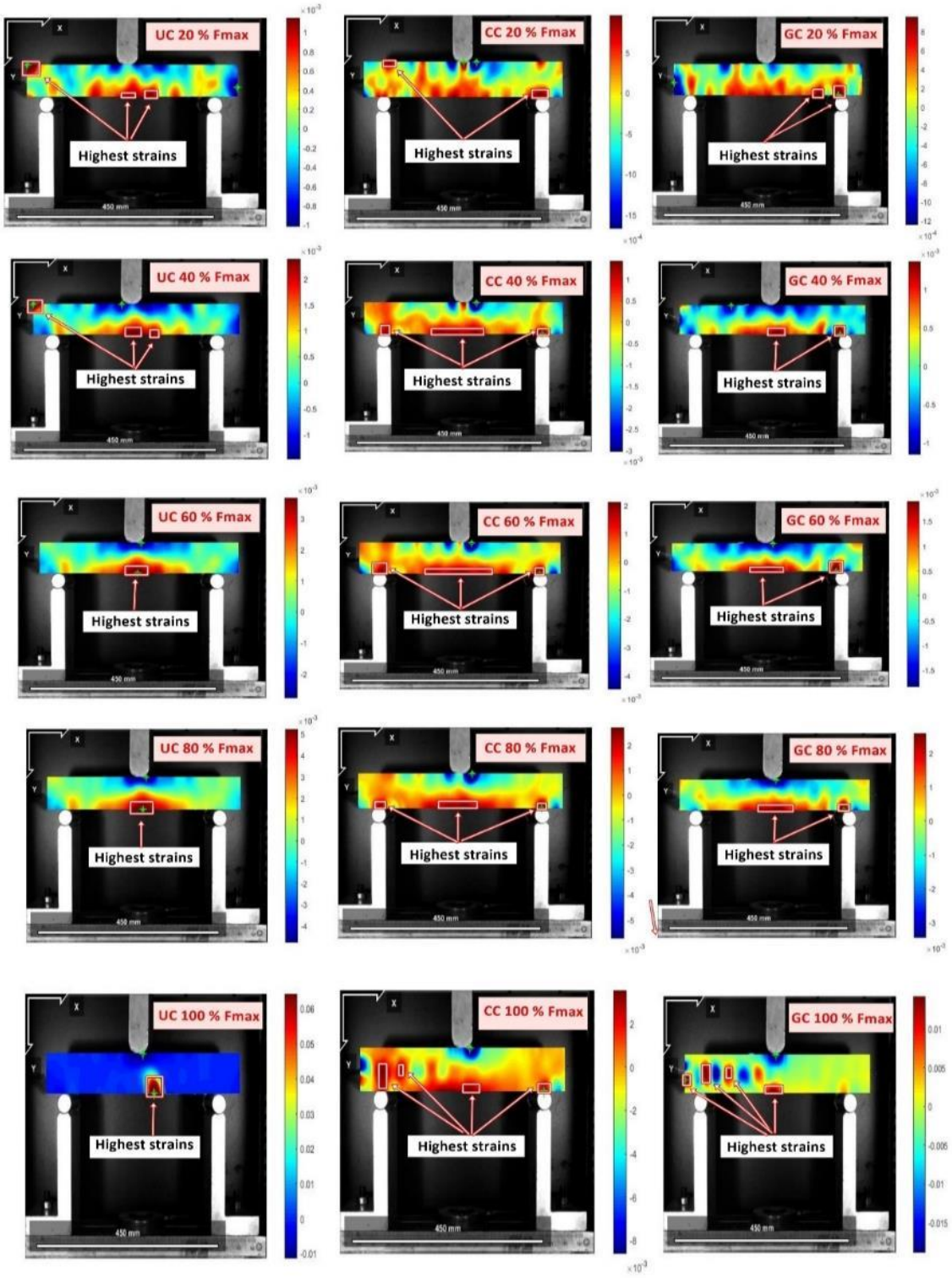

Fig. 4. The ε_{xx} (strain along the x-direction) contours of UC, CC, and GC at different load levels

As can be seen from the curves, the DIC method and experimental results were compatible with each other. In Fig. 3 and Table 4, it was observed that glass reinforced composites decreased the displacement at different load levels (20%, 40%, 60% and 80% of F_{MAX}).

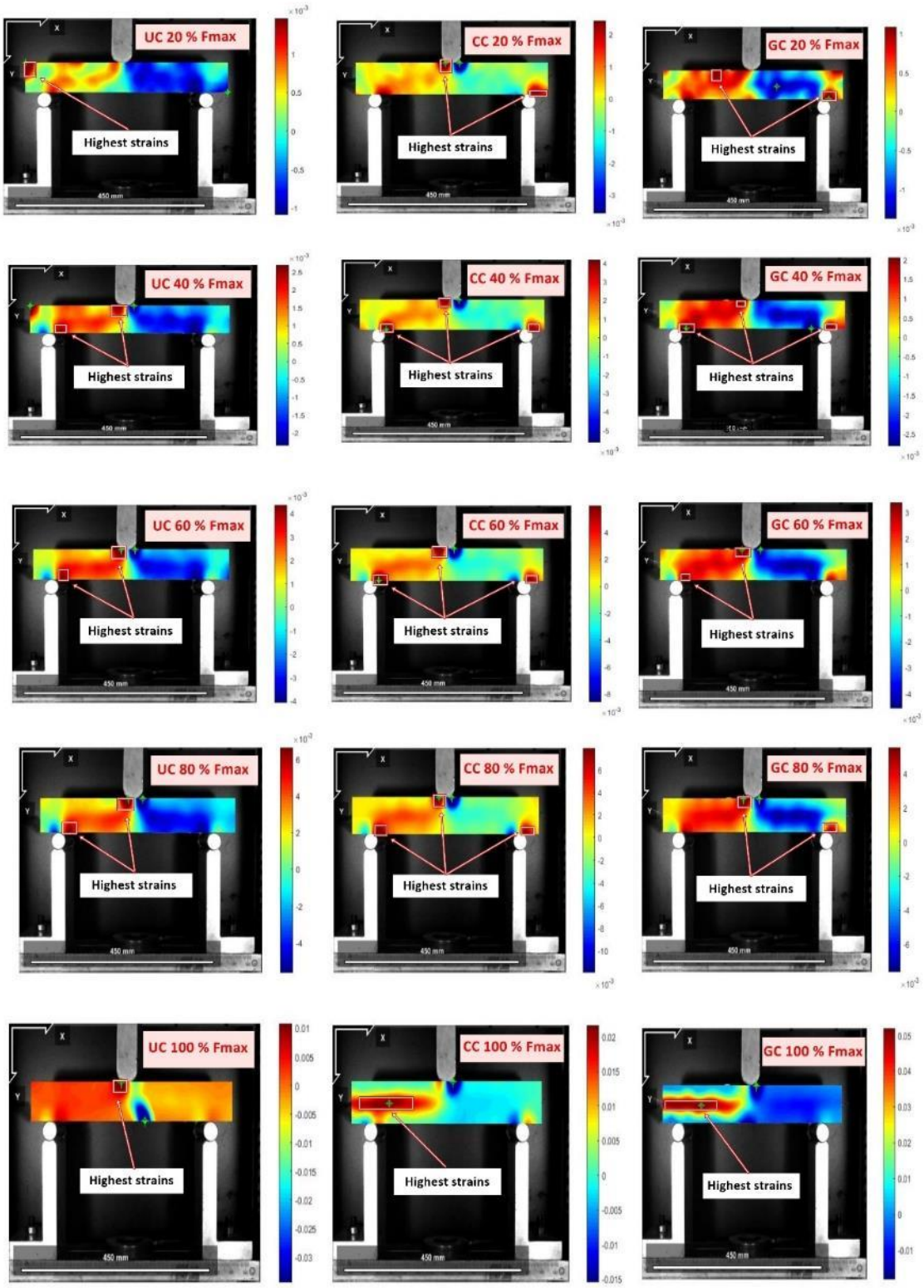

Fig. 5. ε_{xy} (shear strain) contours of UC, CC, and GC at different load levels

In the literature, it has been emphasized that the highest $\mathcal{E}_{xx}$ (strain along the x-direction) contours of composites can be used for tracking crack development at various stages of loading (Suryanto *et al*. 2017). The size and length of the strain contours indicate the progression of existing cracks. Based on the DIC images, cracks begin at the bottom of all composites. After 60% of the maximum load, reinforced and unreinforced composites showed differences. Strain contours in non-reinforced composites concentrated at one point while reinforced composites concentrated at several points. Figure 4 shows $\mathcal{E}_{xx}$ (strain along the x-direction) contours of UC, CC, and GC at different load levels. When examining DIC images in ultimate load, the differences between crack modes were clearly seen in wood composites. The maximum strain contours ($\mathcal{E}_{xx}$) in the unreinforced composites were concentrated in the bottom part. This shows that the failure was in the wood. The maximum strain contours ($\mathcal{E}_{xx}$) in carbon and glass reinforced composites were concentrated on the bottom and left sides. These contours indicate that the failure was caused by the adhesive line and wood. The results indicate that, in the case of improved bonding performance with the reinforcing material, higher strength can obtain in carbon and glass reinforced composites.

Figure 5 shows $\mathcal{E}_{xy}$ (shear strain) contours of UC, CC, and GC at different load levels. The shear stress of carbon and glass reinforced wood composites under maximum load was concentrated on the left side. However, the strain in the unreinforced wood composites was concentrated in the bottom.

The shear strain along adhesive layer was examined under a certain load (60% of the maximum load) to obtain more details on wood composites. Figure 6 shows the shear strain values at 60% load level throughout the adhesive layer of reinforced and unreinforced wood composites.

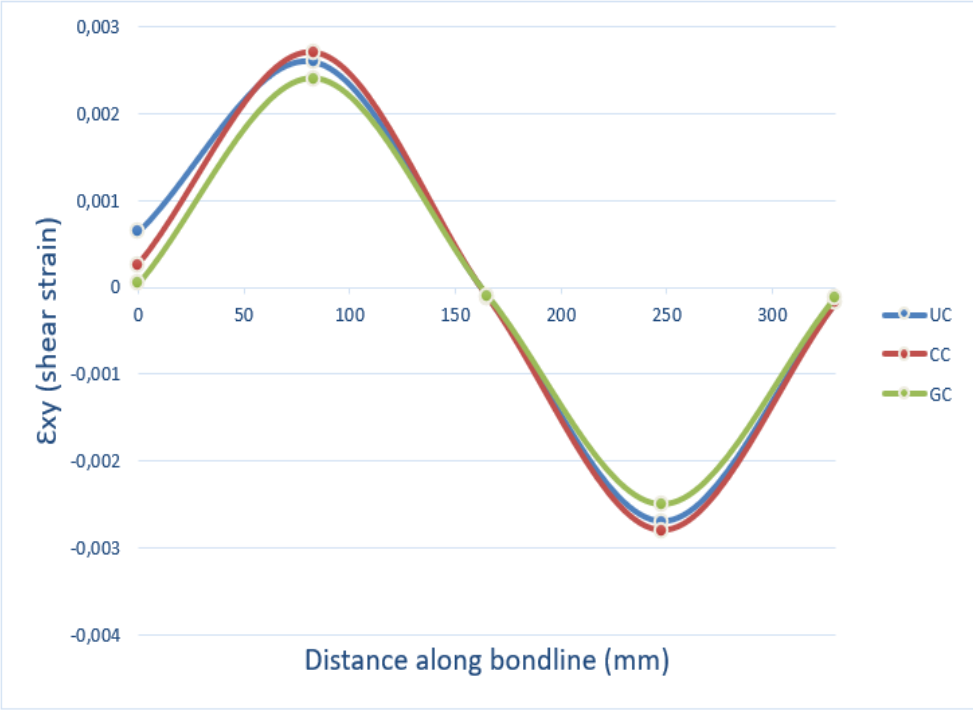

Fig. 6. The shear strain of values at 60% load level in different wood composites

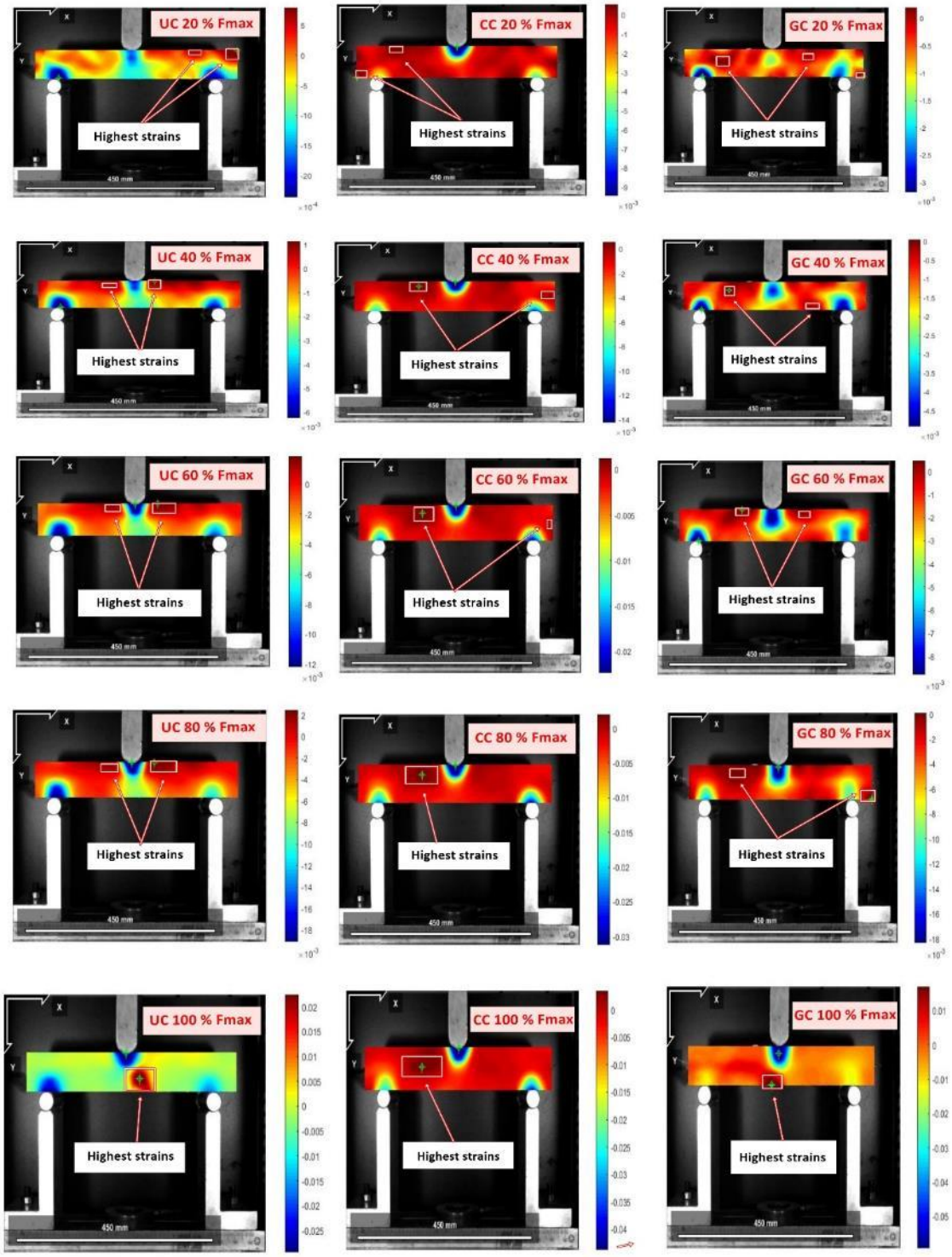

Fig. 7. ε_{yy} (strain along the y-direction) contours of UC, CC, and GC at different load levels

When the adhesive layer was examined, the lowest shear strain values were observed in the glass reinforced wood composites. The results showed that glass fibre has a positive effect on the adhesive line. It has been reported that the smaller the strain value in the adhesive layer means better strength (Guan *et al.* 2014). This is the cause of the highest bending strength of glass-reinforced wood composites. When Table 4 and DIC images are examined, the lowest shear strain values were observed in glass reinforced composites supports this view. The highest strain values were seen in carbon reinforced wood composites.

Figure 7 shows $\mathcal{E}_{yy}$ (strain along the y-direction) contours of UC, CC, and GC at different load levels. In general, it appeared that the stress was distributed more homogeneously in these composites. The strain field along the y-direction was different in the carbon fibre-reinforced composites. Glass reinforced and unreinforced composites showed strain concentrated in the bottom.

The strain field along the y-direction was different in the carbon fibre reinforced composites. In general, the maximum $\mathcal{E}_{yy}$ fields of the carbon fiber reinforced composites were concentrated on the left side while the unreinforced and glass fibre reinforced composites were concentrated in the bottom. The maximum $\mathcal{E}_{yy}$ fields in the glue line of carbon fiber reinforced composites indicate that the carbon fiber and adhesive were a mismatch with each other. When the DIC images were examined, it was found that a large strain area was formed on the left side of the carbon reinforced composites under the ultimate load. This indicates delamination in the adhesive area. The delamination caused by mismatch was thought to be the main reason for the lowest bending strength in carbon fiber reinforced composites.

It is difficult to determine the critical deformations of composite materials under different loads. Conventional methods of deformation measurement are inadequate in some cases. Further information on materials can be achieved through the DIC method. In this study, DIC was successfully used to determine deformation behaviours of different composites. Differences in strain and displacement fields were measured in three different composite materials. The interaction between glue and fibre material could be attributed to the difference in carbon fibre and glass fibre reinforced composites.

CONCLUSIONS

1. The results showed that polyurethane adhesive was not suitable for carbon fibre reinforced wood composites.
2. In carbon fibre reinforced composites, it was found that there is more $\mathcal{E}_{xy}$ (shear strain) in the adhesive line than in other composites.
3. It was determined that the strength of bending was improved significantly in wood composites prepared with glass fiber.
4. DIC method results showed that the type of reinforcement material used in the wood composites produced with polyurethane affects the crack mode.
5. As a result, it was determined that the performance should be improved by paying attention to adhesive compatibility and strain dispersion. It is not sufficient just to add reinforcements to reinforce the wood composite

REFERENCES CITED

Alam, S. Y., Saliba, J., and Loukili, A. (2014). "Fracture examination in concrete through combined digital image correlation and acoustic emission techniques," *Construction and Building Materials* 69, 232-242. DOI: 10.1016/J.CONBUILDMAT.2014.07.044

Bardak, T., Bardak, S., and Sozen E. (2017) "Determination of strain distributions of solid wood and plywood in bending test by digital image correlation," *Kastamonu Univ., Journal of Forestry Faculty* 17, 354-361. DOI: 10.17475/kastorman.328188.

Bigaud, J., Aboura, Z., Martins, A. T., and Verger, S. (2018). "Analysis of the mechanical behavior of composite T-joints reinforced by one side stitching," *Composite Structures* 184, 249-255. DOI: 10.1016/J.COMPSTRUCT.2017.06.041

Blaber, J., Adair, B., and Antoniou, A. (2015). "Ncorr: Open-source 2D digital image correlation Matlab software," *Experimental Mechanics* 55(6), 1105-1122. DOI: 10.1007/s11340-015-0009-1

Caminero, M. A., Lopez-Pedrosa, M., Pinna, C., and Soutis, C. (2014). "Damage assessment of composite structures using digital image correlation," *Applied Composite Materials* 21(1), 91-106. DOI: 10.1007/s10443-013-9352-5

Dunlop, J. W. C., and Fratzl, P. (2013). "Multilevel architectures in natural materials," *Scripta Materialia* 68(1), 8-12. DOI: 10.1016/J.SCRIPTAMAT.2012.05.045

Guan, M., Yong, C., and Wang, L. (2014). "Microscopic characterization of modified phenol-formaldehyde resin penetration of bamboo surfaces and its effect on some properties of two-ply bamboo bonding interface," *BioResources* 9(2), 1953-1963. DOI: 10.15376/biores.9.2.1953-1963

Harilal, R., Vyasarayani, C. P., and Ramji, M. (2015). "A linear least squares approach for evaluation of crack tip stress field parameters using DIC," *Optics and Lasers in Engineering* 75, 95-102. DOI: 10.1016/j.optlaseng.2015.07.004

Hryniewicz, P., Banaś, W., Gwiazda, A., Foit, K., Sękala, A., and Kost, G. (2015). "Technological process supervising using vision systems cooperating with the LabVIEW vision builder," *IOP Conference Series: Materials Science and Engineering* 95(1). DOI: 10.1088/1757-899X/95/1/012086

Hu, M., Johansson, M., Olsson, A., Oscarsson, J., and Enquist, B. (2015). "Local variation of modulus of elasticity in timber determined on the basis of non-contact deformation measurement and scanned fibre orientation," *European Journal of Wood and Wood Products* 73(1), 17-27. DOI: 10.1007/s00107-014-0851-3

Ianasi, A. C. (2015). "On the role of CFRP reinforcement for wood beams stiffness," *IOP Conference Series: Materials Science and Engineering* 95(1). DOI: 10.1088/1757-899X/95/1/012015

Jeong, G. Y., and Park, M. J. (2016). "Evaluate orthotropic properties of wood using digital image correlation," *Construction and Building Materials* 113, 864-869. DOI: 10.1016/J.CONBUILDMAT.2016.03.129

Li, L., Gong, M., Chui, Y. H., Schneider, M., and Li, D. (2013). "Measurement of the elastic parameters of densified balsam fir wood in the radial-tangential plane using a digital image correlation (DIC) method," *Journal of Materials Science* 48(21), 7728-7735. DOI: 10.1007/s10853-013-7593-1

Ling, H., Samarasinghe, S., and Kulasiri, G. D. (2009). "Modelling variability in full-field displacement profiles and Poisson ratio of wood in compression using stochastic neural networks," *Silva Fennica* 43(5), 871-887. DOI: 10.14214/sf.460

Ljungdahl, J., Berglund, L. A., and Burman, M. (2006). "Transverse anisotropy of

compressive failure in European oak – A digital speckle photography study," *Holzforschung* 60(2), 190-195. DOI: 10.1515/HF.2006.031

Luo, P. F., Chao, Y. J., Sutton, M. A., and Peters, W. H. (1993). "Accurate measurement of three-dimensional deformations in deformable and rigid bodies using computer vision," *Experimental Mechanics* 33(2), 123-132. DOI: 10.1007/BF02322488

Mahal, M., Blanksvärd, T., Täljsten, B., and Sas, G. (2015). "Using digital image correlation to evaluate fatigue behavior of strengthened reinforced concrete beams," *Engineering Structures* 105, 277-288. DOI: 10.1016/J.ENGSTRUCT.2015.10.017

Mahmoodi, M., James, L. A., and Johansen, T. (2018). "Automated advanced image processing for micromodel flow experiments; an application using labVIEW," *Journal of Petroleum Science and Engineering* 167, 829-843. DOI: 10.1016/J.PETROL.2018.02.031

Nguyen, V.-T., Kwon, S.-J., Kwon, O.-H., and Kim, Y.-S. (2017). "Mechanical properties identification of sheet metals by 2D-digital image correlation method," *Procedia Engineering* 184, 381-389. DOI: 10.1016/J.PROENG.2017.04.108

Pan, B., Qian, K., Xie, H., and Asundi, A. (2009). "Two-dimensional digital image correlation for in-plane displacement and strain measurement: A review," *Measurement Science and Technology*, 20(6). DOI: 10.1088/0957-0233/20/6/062001

Serrano, E., and Enquist, B. (2005). "Contact-free measurement and non-linear finite element analyses of strain distribution along wood adhesive bonds," *Holzforschung* 59(6), 641-646. DOI: 10.1515/HF.2005.103

Shen, M., Touchard, F., Bezine, G., and Brillaud, J. (2015). "Direct numerical simulation of fracture behaviour for random short wood fibre-reinforced composites in comparison with digital image correlation experiments," *Journal of Thermoplastic Composite Materials* 28(5), 686-704. DOI: 10.1177/0892705713489324

Sjödin, J., Enquist, B., and Serrano, E. (2006). "Contact-free measurements and numerical analyses of the strain distribution in the joint area of steel-to-timber dowel joints," *Holz als Roh- und Werkstoff* 64(6), 497-506. DOI: 10.1007/s00107-006-0112-1

Suryanto, B., Tambusay, A., and Suprobo, P. (2017). "Crack mapping on shear-critical reinforced concrete beams using an open source digital image correlation software," *Civil Engineering Dimension* 19(2), 93-98. DOI: 10.9744/ced.19.2.93-98

Sutton, M. A., McNeill, S. R., Jang, J., and Babai, M. (1988). "Effects of subpixel image restoration on digital correlation error estimates," *Optical Engineering* 27(10), 271070. DOI: 10.1117/12.7976778

Tavakkolizadeh, M., and Saadatmanesh, H. (2001). "Galvanic corrosion of carbon and steel in aggressive environments," *Journal of Composites for Construction* 5(3), 200-210. DOI: 10.1061/(ASCE)1090-0268(2001)5:3(200)

Tekieli, M., De Santis, S., de Felice, G., Kwiecień, A., and Roscini, F. (2017). "Application of digital image correlation to composite reinforcements testing," *Composite Structures* 160, 670-688. DOI: 10.1016/J.COMPSTRUCT.2016.10.096

Thorhallsson, E. R., Hinriksson, G. I., and Snæbjörnsson, J. T. (2017). "Strength and stiffness of glulam beams reinforced with glass and basalt fibres," *Composites Part B: Engineering* 115, 300-307. DOI: 10.1016/J.COMPOSITESB.2016.09.074

TS 2474 (1976). "Wood - Determination of ultimate strength in static bending," Turkish Standards Institution, Ankara, Turkey.

Valle, V., Laou, L., Léandry, I., Yotte, S., Rossignol, S., and Hedan, S. (2018). "Crack analysis in mudbricks under compression using specific development of stereo-digital

image correlation," *Experimental Mechanics* 58(3), 475-486. DOI: 10.1007/s11340-017-0363-2

Vora, S. R., Bognet, B., Patanwala, H. S., Young, C. D., Chang, S.-Y., Daux, V., and Ma, A. W. K. (2018). "Global strain field mapping of a particle-laden interface using digital image correlation," *Journal of Colloid and Interface Science* 509, 94-101. DOI: 10.1016/J.JCIS.2017.08.082

Wei, P., Wang, B. J., Zhou, D., Dai, C., Wang, Q., and Huang, S. (2013). "Mechanical properties of poplar laminated veneer lumber modified by carbon fiber reinforced polymer," *BioResources* 8(4), 4883-4898. DOI: 10.15376/biores.8.4.4883-4898

Yoneyama, S., Koyanagi, J., and Arikawa, S. (2016). "Measurement of discontinuous displacement/strain using mesh-based digital image correlation," *Advanced Composite Materials* 25(4), 329-343. DOI: 10.1080/09243046.2015.1052131

Zhou, A., Tam, L.-h., Yu, Z., and Lau, D. (2015). "Effect of moisture on the mechanical properties of CFRP–wood composite: An experimental and atomistic investigation," *Composites Part B: Engineering* 71, 63-73. DOI: 10.1016/J.COMPOSITESB.2014.10.051

Article submitted: July 5, 2018; Peer review completed: October 11, 2018; Revised version received: November 6, 2018; Accepted: November 7, 2018; Published: November 14, 2018.
DOI: 10.15376/biores.14.1.180-192